

# Characterizing the Adhesion of Motile and Nonmotile *Escherichia coli* to a Glass Surface Using a Parallel-Plate Flow Chamber

Jennifer W. McClaine, Roseanne M. Ford

Department of Chemical Engineering, University of Virginia, 102 Engineers' Way, P.O. Box 400741, Charlottesville, Virginia 22904-4741, USA; telephone: 434-924-6283; fax: 434-982-2658; e-mail: rmf3f@virginia.edu

Received 5 February 2001; accepted 9 November 2001

**Abstract:** A parallel-plate flow chamber was used to measure the attachment and detachment rates of *Escherichia coli* to a glass surface at various fluid velocities. The effect of flagella on adhesion was investigated by performing experiments with several *E. coli* strains: AW405 (motile); HCB136 (nonmotile mutant with paralyzed flagella); and HCB137 (nonmotile mutant without flagella). We compared the total attachment rates and the fraction of bacteria retained on the surface to determine how the presence and movement of the flagella influence transport to the surface and adhesion strength in this dynamic system. At the lower fluid velocities, there was no significant difference in the total attachment rates for the three bacterial strains; nonmotile strains settled at a rate that was of the same order of magnitude as the diffusion rate of the motile strain. At the highest fluid velocity, the effect of settling was minimized to better illustrate the importance of motility, and the attachment rates of both nonmotile strains were approximately five times slower than that of the motile bacteria. Thus, different processes controlled the attachment rate depending on the parameter regime in which the experiment was performed. The fractions of motile bacteria retained on the glass surface increased with increasing velocity, whereas the opposite trend was found for the nonmotile strains. This suggests that the rotation of the flagella enables cells to detach from the surface (at the lower fluid velocities) and strengthens adhesion (at higher fluid velocities), whereas nonmotile cells detach as a result of shear. There was no significant difference in the initial attachment rates of the two nonmotile species, which suggests that merely the presence of flagella was not important in this stage of biofilm development. © 2002 Wiley Periodicals, Inc. *Biotechnol Bioeng* 78: 179–189, 2002; DOI 10.1002/bit.10192

**Keywords:** *Escherichia coli*; motility; flagella; adhesion; flow chamber

## INTRODUCTION

The attachment of bacteria to surfaces is the first step in biofilm formation (Costerton et al., 1987; Lawrence

et al., 1987). Biofilms can be both beneficial and detrimental; that is, they can be essential to the operation of wastewater treatment facilities, septic systems, and bioremediation schemes (Witt et al., 1999), or can lead to serious disease when formed on the surface of medical implants (Gristina, 1987), teeth (Characklis and Marshall, 1990), or on the interior of lungs (Feldman et al., 1998). In bioremediation, bacteria and nutrients are injected into a contaminated region and move through the soil with groundwater flow. Bacteria attach to and detach from soil particles within the porous matrix, and with appropriate nutrients grow to form biofilms on the soil surfaces. These biofilms form a reaction zone in which contaminants in the incoming groundwater are degraded, and are therefore essential to a successful bioremediation scheme.

A physical parameter important in the attachment of bacteria to surfaces is the velocity of the carrier fluid. As the fluid velocity is increased, bacteria have less time to interact with the surface and therefore attach at a relatively slower rate. At the same time, increasing the velocity also enables a larger number of bacteria to pass over the surface in a given time period, a phenomenon that tends to have the opposite effect. A significant amount of research has been done to better understand the effect of fluid velocity on the adhesion of nonmotile bacteria, involving both specific (Dickinson and Cooper, 1995; Mohamed et al., 1999, 2000) and nonspecific (Gannon et al., 1991; Gross and Logan, 1995; Meinders et al., 1992, 1994; Wollum and Cassel, 1978) interactions. However, because approximately 80% of bacteria studied so far are motile (Aizawa, 1996), we are primarily interested in understanding how fluid velocity affects the transport and adhesion of motile bacteria in comparison to their nonmotile counterparts.

The swimming behavior of motile bacteria may allow a population to spread out more effectively than a nonmotile bacterial population, especially in directions perpendicular to fluid flow where dispersion is minimal (Harvey, 1991). This may be important in bioremedia-

Correspondence to: R. Ford

Contract grant sponsor: National Science Foundation

Contract grant number: BES-9809388

tion schemes involving multiple injection wells (McMurtry and Elton, 1985; Starr and Cherry, 1994), because motility would allow the cells to distribute more uniformly between injection wells and grow to form a more continuous biofilm.

Motility has also been found to affect the adhesion of bacteria to various surfaces in flowing systems, including glass (Korber et al., 1994; Mueller, 1996) and stainless steel (Mueller, 1996) in flow chambers, and soil (Camesano and Logan, 1998) and glass beads (Camper et al., 1993) in packed columns. Mueller (1996) compared the attachment rates of motile and nonflagellate *Pseudomonas fluorescens* CC-840406-E to various surfaces in a flow chamber at an average fluid velocity of  $2.75 \text{ cm s}^{-1}$ . The attachment rate of motile cells was approximately 1.5, 2, and 3-fold higher than nonflagellate cells for the stainless steel, polycarbonate, and glass surfaces, respectively. Similar results were reported by Camper et al. (1993) and Korber et al. (1994) for the attachment of the same bacterial species to a glass surface within a flow chamber using average fluid velocities of  $2.75 \text{ cm s}^{-1}$  and  $0.37 \text{ cm s}^{-1}$ . Korber et al. (1994) also performed experiments with heat-treated *P. fluorescens* to determine whether the discrepancy in attachment rates could be attributed to functionality of the flagellum. Heat-treated cells (i.e., motile cells rendered nonmotile) attached at rates similar to nonflagellate cells, at an average fluid velocity of  $0.37 \text{ cm s}^{-1}$ .

In experiments performed with columns packed with glass beads, Camper et al. (1993) saw no marked effect of motility in the breakthrough curves of motile and nonflagellate *P. fluorescens* at a pore velocities of  $0.0028 \text{ cm s}^{-1}$  and  $0.0125 \text{ cm s}^{-1}$  (in terms of peak height position, time to initial breakthrough, and cell recovery). At a velocity of  $0.00057 \text{ cm s}^{-1}$ , the amount of motile cells retained in the column was significantly higher than the number of nonflagellate cells. This is inconsistent with results reported by Camesano and Logan (1998), who measured the fraction of motile and nonmotile (killed) *Pseudomonas fluorescens* P17 retained in soil columns over the interstitial velocity range of  $0.00065$  to  $0.14 \text{ cm s}^{-1}$ . At flow rates less than approximately  $0.0625 \text{ cm s}^{-1}$ , the fraction of motile bacteria retained in the columns was significantly lower in comparison to nonmotile bacteria, and at higher fluid velocities the motile and nonmotile bacteria were retained in similar numbers. Thus, the importance of motility in dynamic adhesion and its dependence on the fluid velocity is not well understood.

The specific role of the flagella in biofilm formation has also been studied in stagnant systems (O'Toole and Kolter, 1998a, 1998b; Pratt and Kolter, 1998; Watnick and Kolter, 1999). Pratt and Kolter (1998) found that motility was essential for normal biofilm formation (using *E. coli* and various plastic surfaces), and suggested that the role of motility was to promote bacterial

adhesion and allow cells to spread out across the surface. Nonflagellate and paralyzed *E. coli* cells were unable to develop biofilms because they attached in much smaller numbers and were incapable of expanding individual microcolonies to form a continuous biofilm (Pratt and Kolter, 1998). Furthermore, there was no difference in the rate of biofilm formation between cells with and without flagella in the absence of motility (Pratt and Kolter, 1998). Similar results were found studying the adhesion and growth of *Pseudomonas aeruginosa* PA14 (O'Toole and Kolter, 1998a) and *Vibrio cholerae* El Tor (Watnick and Kolter, 1999) on polyvinylchloride (PVC) surfaces. Vatanyoopaisarn et al. (2000), however, found that the initial attachment of paralyzed *Listeria monocytogenes* to stainless steel was ten times higher than nonflagellate cells.

In this study, we investigate the effect of fluid velocity on the attachment and detachment of motile and nonmotile bacteria to glass surfaces using a parallel-plate flow chamber. We examined several possible roles of the flagella: enabling more bacterial cells to reach the surface from the bulk and consequently attach in greater numbers (by comparing total and net attachment rates of motile bacteria with paralyzed or nonflagellate strains); giving attached cells a mechanism for detachment (by comparison of fractions retained of motile bacteria with paralyzed or nonflagellate strains); or increasing the strength of adhesion (by comparison of fractions retained of paralyzed with nonflagellate strains).

## MATERIALS AND METHODS

### Bacteria and Growth Conditions

The bacteria used in this study were *Escherichia coli* K12 AW405 (motile with ~5 to 10 flagella [Macnab, 1996]), *Escherichia coli* K12 HCB137 (nonmotile without flagella), and *Escherichia coli* K12 HCB136 (nonmotile with paralyzed flagella). Bacteria were grown from frozen stock on a rotary shaker (Orbit Environ-shaker, Lab-Line Instruments, Inc.) in 100 mL of tryptone broth to optical densities of 1.0 (measured at 590 nm and corresponding to the late exponential phase). Cells were resuspended in filter-sterilized random motility buffer to a concentration of  $(5 \pm 2) \times 10^6 \text{ cells mL}^{-1}$ . This concentration was sufficiently low to neglect cell-cell interactions and corresponded to 20 to 150 cells/viewing area. Bacterial cells were left in buffer for approximately 1 to 1.5 h prior to experiments to ensure that cell division had ceased.

Tryptone broth contains 5 g NaCl and 10 g tryptone (Difco 0123-17-3) per liter of filtered, deionized water. Random motility buffer contains 11.2 g  $\text{KH}_2\text{PO}_4$ , 4.8 g  $\text{K}_2\text{HPO}_4$ , and 0.029 g ethylene-diamine tetraacetic acid (EDTA) per liter of filtered, deionized water. The ionic strength of this buffer is 0.2 M.

## Flow Chamber and Data Analysis

The parallel-plate flow chamber (PPFC) consists of a Plexiglas block (3 cm × 5.8 cm), a silastic gasket (Sil-Tec medical-grade sheeting, Technical Products, Inc. of Georgia), and a glass microscope slide (Fisher Scientific, Catalog # 12-550B) held together by vacuum (Fig. 1). The center of the Plexiglas block comprises the top of the chamber (3 cm × 1 cm), and contains fluid entrance and exit slits at opposite ends. The slits are connected to inlet and outlet ports located on one side of the block. A groove (4 mm wide × 1 mm deep) surrounds the top of the chamber and is connected to the vacuum port. A thin film of vacuum grease is applied around the edge of the chamber top to ensure a tight seal. The silastic gasket (5.8 cm × 3 cm × 0.102 cm, with opening 3 cm × 1 cm) is placed against the Plexiglas block so that the top of the chamber and the opening in the center of the gasket are aligned; small holes in the gasket directly below the groove facilitate vacuum communication. The bottom of the chamber is a glass microscope slide (75 mm × 38 mm). The microscope slides used in experiments were cleaned with detergent (Sparkleen, Fisher Scientific) prior to flow chamber assembly, scrubbing well with a toothbrush. The slides were then rinsed thoroughly with tap water (with a final rinse of DI water), and dried with compressed air. We used a new microscope slide for each experiment. The overall dimensions of the chamber are 1 cm × 3 cm × 0.0762 cm. The viewing area is 0.0625 mm<sup>2</sup> and the depth of field is approximately 10 μm.

The entire flow chamber was placed on the stage of an inverted microscope (phase objective; Nikon TMS)

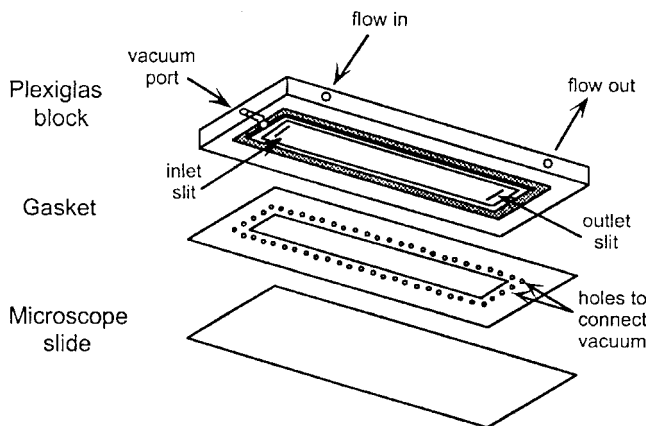


**Figure 1.** Diagram of the parallel-plate flow chamber used in the experiments. The top of the chamber is a Plexiglas block that has entrance and exit slits located on opposite ends to allow for fluid flow. These slits are connected to the inlet and outlet ports located on the side of the Plexiglas block. The thickness of the chamber is determined by the silastic gasket, which is pressed against the Plexiglas block so that the holes are directly over the shaded groove, which is in turn connected to the vacuum port. A thin layer of vacuum grease is applied between the Plexiglas block and gasket around the chamber top to ensure a tight seal. The bottom of the chamber is a glass microscope slide.

equipped with a 40× ultra-long working distance objective. A CCD camera (Dage MTI CCD72) was mounted to the top of the microscope and connected to a TV screen (Sony) and Macintosh G4 computer.

Approximately 40 pore volumes of buffer were first pumped through the chamber using a syringe pump (Harvard Apparatus PHD 2000) to equilibrate the system. (One pore volume was defined as the volume of fluid necessary to fill the flow chamber, 0.23 cm<sup>3</sup>.) Care was taken to ensure no air bubbles remain trapped within the flow chamber. A dilute bacterial suspension ( $5 \pm 2 \times 10^6$  cells/mL) was then pumped through the flow chamber at the desired flow rate. Two snapshots of a specific viewing area located in the center of the chamber ( $x = 1.5$  cm) were taken approximately 4 s apart at regular intervals using VIDEO IMPRESSION (Global Village). The set of two snapshots was necessary to differentiate between attached cells and cells moving near the surface. Attached bacteria were defined as bacteria that remained in the same location for two consecutive snapshots; that is, cells that attached to the surface for at least 4 s. Note that we varied the time between snapshots from approximately 2 to 10 s without any significant change in attached bacteria; we chose 4 s from within that range for our experiments. To eliminate artifacts caused by dust on the lens and camera, a background image was subtracted from all snapshots prior to analysis. Cells that attached and detached were then counted manually using NIH IMAGE 1.44 and plotted as a function of time.

## Total Cell Counts

Samples of the bacteria/buffer solution were stored at the beginning and end of each experiment to determine the average bulk concentration of bacteria within the chamber. One milliliter of the cell suspension was preserved in 5 mL of 3% (v/v) formaldehyde and refrigerated. AO counts were performed as described by Hobbie et al. (1977). Two or three counts were performed per sample, and each count represented an average of ten fields per filter.

## THEORETICAL ASPECTS

A general expression for the two-dimensional transport of aqueous phase bacteria through the flow chamber (Fig. 2) is described by the following macroscopic conservation equation:

$$\frac{\partial c}{\partial t} = D_b \frac{\partial^2 c}{\partial y^2} - \frac{\partial(v_s c)}{\partial y} + D_b \frac{\partial^2 c}{\partial x^2} - v \frac{\partial c}{\partial x} \quad (1)$$

where  $c$  is the concentration of bacteria,  $t$  is time,  $x$  is the axial direction,  $y$  is the direction perpendicular to flow,

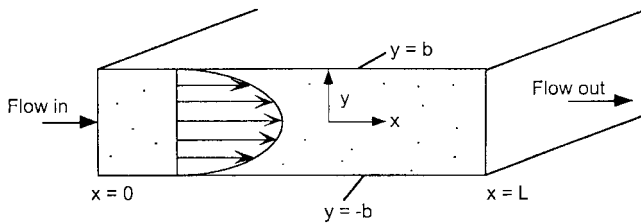


**Figure 2.** A side-view of the parallel plate flow chamber for mathematical purposes. The center of the chamber is located at  $y = 0$ , and the chamber half-height corresponds to  $y = b$ . The chamber inlet ( $x = 0$ ) and outlet ( $x = L$ ) are also shown. The velocity profile within the chamber is parabolic.

$D_b$  is the bacterial diffusion (or random motility) coefficient,  $v_s$  is the settling velocity, and  $v$  is the fluid velocity. The fluid velocity inside the chamber follows a parabolic profile:

$$v = \frac{3}{2}u \left[ 1 - \left( \frac{y}{b} \right)^2 \right] \quad (2)$$

where  $b$  is the chamber half-height and  $u$  is the average fluid velocity. This expression was derived from a momentum balance, assuming a Newtonian fluid with constant density and no-slip boundary conditions.

The diffusion coefficient of a nonmotile, rod-shaped bacterium can be estimated by (Berg, 1993):

$$D_b = \frac{kT}{6\pi\mu a_b} \ln \left( \frac{2a_b}{b_b} \right) \quad (3)$$

where  $k$  is the Boltzmann constant ( $1.38 \times 10^{-16} \text{ g} \cdot \text{cm}^2 \text{ s}^{-2} \text{ K}^{-1}$ ),  $T$  is the absolute temperature (298 K),  $\mu$  is the fluid viscosity ( $0.0098 \text{ g cm}^{-1} \text{ s}^{-1}$ ), and  $a_b$  and  $b_b$  are the half-height and half-width of the bacterium, respectively. If we assume the diameter of a bacterium is approximately  $1 \mu\text{m}$  ( $b_b = 0.5 \mu\text{m}$ ) and length is  $2 \mu\text{m}$  ( $a_b = 1 \mu\text{m}$ ), we estimate a diffusion coefficient of  $3 \times 10^{-9} \text{ cm}^2 \text{ s}^{-1}$ . The random motility coefficient of (motile) *E. coli* AW405 is reported to be  $2.9 \times 10^{-6} \text{ cm}^2 \text{ s}^{-1}$  (Lewus and Ford, 2001).

If axial diffusion and settling are negligible, the steady-state solution to Eq. (1) is given by (Bowen et al., 1976):

$$J_y = \frac{c_o D_b}{b} \frac{\left( \frac{2}{9\gamma} \right)^{1/3}}{\Gamma(4/3) + \frac{D_b}{k_a b} \left( \frac{2}{9\gamma} \right)^{1/3}} \quad (4)$$

where  $J_y$  is the flux to the surface,  $c_o$  is the bulk concentration of bacteria,  $\gamma$  is equal to  $(1/\text{Pe})(8x/3b)$ , the Peclet number ( $\text{Pe}$ ) is equal to  $4ub/D_b$ ,  $x$  is the axial position,  $k_a$  is the first-order adsorption rate constant, and is the gamma function [ $\Gamma(4/3) = 0.89338$ ]. This

solution is appropriate for large  $\text{Pe}$  values, and requires that we assume all concentration differences occur in a thin layer above the surface where the fluid velocity can be approximated as linear. Thus, we approximate the walls as infinitely separated. Under the conditions of our experiments, the Peclet number ranged between 200 and  $2 \times 10^5$ , satisfying the large  $\text{Pe}$  condition. Further details of the mathematical solution were given by Bowen et al. (1976). It should also be noted that this flux expression does not take into account the reduction of the velocity of a bacterium moving with the fluid due to its proximity to the solid surface (Goldman et al., 1967).

We relate experimental data to the flux expression with:

$$N_b = J_y A_v t \quad (5)$$

where  $N_b$  is the number bacteria observed at a given time  $t$  within the viewing area,  $A_v$  ( $6.25 \times 10^{-4} \text{ cm}^2$ ).

A limitation to this model [Eq. (4)] is that the boundary condition at the surface (diffusion rate equals adsorption rate) does not include the detachment of cells. Because we are able to measure experimentally both the total number of cells that interact with the surface and the net attached (total cells minus detached cells), it is useful to define the fraction retained on the surface,  $F_R$ , as:

$$F_R = \frac{J_{y,\text{net}}}{J_{y,\text{total}}} \quad (6)$$

where  $J_{y,\text{net}}$  is the flux measured from the net bacteria accumulated on the surface and  $J_{y,\text{total}}$  is the flux measured from the total bacteria that have interacted with the surface, including those that have detached. We also refer to the total attachment rate, defined as  $J_{y,\text{tot}}/c_o$ .

### Settling Velocity

An expression for the settling velocity of a nonmotile, rod-shaped bacterium can be determined from a force balance in the absence of fluid flow, including terms to account for the effects of gravity, buoyancy, and drag, respectively (Bird et al., 1960):

$$\rho_s V g = \rho_f V g + \lambda v_s f \quad (7)$$

where  $\rho_s$  is the density of a bacterium,  $V$  is the volume of a bacterium (equal to  $4/3\pi b_b^2 a_b$  for an ellipsoid),  $g$  is the gravitational constant,  $v_s$  is the settling velocity,  $f$  is the friction factor [equal to  $6\pi\mu a/(\ln(2a_b/b_b))$ ] for an ellipsoid-shaped bacterium moving at random (Berg, 1993), and  $\lambda$  is a correction factor that accounts for the prox-

imity of a solid surface, ranging between one (bulk fluid) and infinity (at the solid surface) (Brenner, 1961).

Substituting the expressions for volume and friction factor into Eq. (7), and rearranging to solve for the settling velocity yields:

$$v_s = \frac{4/3\pi b_b^2 a_b (\rho_s - \rho_f) g}{6\pi\mu a_b \lambda} \ln \frac{2a_b}{b_b} \quad (8)$$

We estimated the size of *E. coli* to be approximately 1  $\mu\text{m}$  in diameter and 2  $\mu\text{m}$  in length (Berg, 1993), with a density between 1.01 and 1.05  $\text{g cm}^{-3}$  (Harvey, 1993). The suspension buffer had properties similar to water at 25°C:  $\rho_f = 0.997 \text{ g cm}^{-3}$ ,  $\mu = 0.0098 \text{ g cm}^{-1} \text{ s}^{-1}$ . For the bulk fluid ( $\lambda = 1$ ), we calculated the settling velocity to be between 0.0052 and 0.021  $\text{cm h}^{-1}$ .

We also determined the settling velocity experimentally by measuring the rate of attachment under no-flow conditions. Specifically, cells were pumped through the flow chamber at 2  $\text{mL min}^{-1}$  for several minutes, and then flow was turned off to allow cells to settle in the absence of fluid flow. The settling rate was determined by counting the number of cells near the surface (those in focus within the depth of field but not necessarily attached) as a function of time. Because the diffusion rate for nonmotile cells was negligible compared with the settling rate in the absence of flow, the flux to the surface was dominated by gravitational settling, and thus  $J_y$  in Eq. (5) was equal to  $v_s c_o$ . Using this method, we determined the settling velocity of nonmotile cells to be approximately  $0.025 \pm 0.003 \text{ cm h}^{-1}$ . [Using Eq. (8) and the parameters given in the previous paragraph, this corresponds to a cell density of 1.09  $\text{g cm}^{-3}$ .] This value may be larger than theoretical because the concentration of cells within the 10- $\mu\text{m}$  region above the surface is slightly higher than that in the bulk (Mohamed et al., 1999). A better approximation would be to assume the flux of cells to the surface was equal to the settling velocity multiplied by the concentration of cells near the surface. A problem with this method is that the surface concentration is difficult to measure; therefore, we chose to use the bulk concentration in our analysis. However, because the surface concentration will be greater than the bulk concentration, the value for the settling velocity reported herein is on the high end. Thus, the density of a bacterium is most likely lower than our estimate of 1.09

$\text{g cm}^{-3}$ . The discrepancy between theoretical and experimental values for the settling velocity may also reflect some uncertainty in parameter estimation in Eq. (8) (e.g., the size and shape of bacterial cells).

For the motile *E. coli* (AW405), we assume the settling velocity is small in comparison to the cell swimming speed of approximately 20  $\mu\text{m s}^{-1}$  (Lewus and Ford, 2001).

## RESULTS

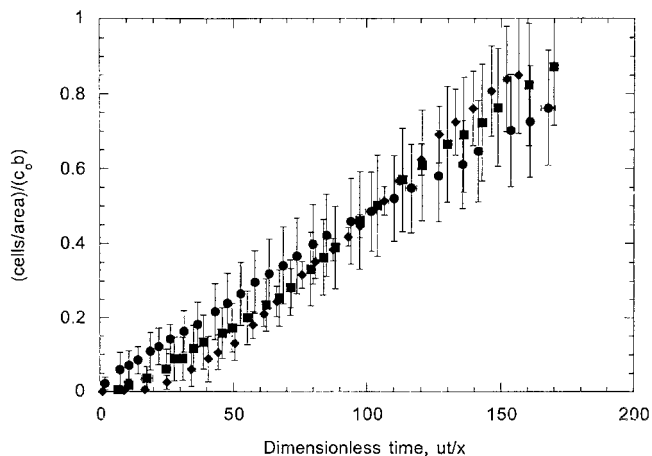
We measured the attachment and detachment rates of motile (AW405), paralyzed (HCB136), and nonflagellate (HCB137) *E. coli* to a glass surface for three average fluid velocities:  $4.4 \times 10^{-1} \text{ cm s}^{-1}$ ,  $4.4 \times 10^{-2} \text{ cm s}^{-1}$ , and  $4.4 \times 10^{-3} \text{ cm s}^{-1}$ . As we increased the fluid velocity, a greater number of bacteria passed by the surface in a given period of time, which artificially increased the number attaching in a given time. To eliminate this effect, we normalized our experimental data by multiplying time by the fluid velocity and dividing by the axial position (similar to a pore volume). We also divided the number of attached cells by the bulk concentration, viewing area, and chamber half-height to nondimensionalize bacterial concentration. A dimensional attachment rate (with units of length per time) can be obtained by multiplying the slope of experimental data by  $ub/x$ . We then compared the fraction of bacteria retained on the surface and rates of net and total accumulation on the surface to determine the effect of motility and the presence of flagella on adhesion.

Figure 3 shows the total attachment rate of the motile, paralyzed, and nonflagellate strains at the flow rate of 0.2  $\text{mL min}^{-1}$ . The figure shows that, at this flow rate, there was no significant difference in the total attachment rates ( $J_{y,\text{tot}}/c_o$ ) of the three bacterial strains ( $0.018 \pm 0.0009 \text{ cm h}^{-1}$ ,  $0.023 \pm 0.005 \text{ cm h}^{-1}$ ,  $0.025 \pm 0.004 \text{ cm h}^{-1}$  for motile, paralyzed, and nonflagellate bacterial strains, respectively). However, we did find that the fraction retained on the surface was significantly lower for both nonmotile species as compared with motile bacteria (Table I). The  $F_R$  for motile bacteria was  $0.70 \pm 0.08$ , compared with  $0.45 \pm 0.07$  and  $0.53 \pm 0.05$  for paralyzed and nonflagellate bacteria, respectively. At the lowest flow rate, 0.02  $\text{mL min}^{-1}$ , there was also no statistical difference in the total attachment rate of the

**Table I.** The fraction of bacteria retained ( $F_R$ ) on a glass surface at various flow rates.

|  | Fraction retained         |                          |                          |
|--|---------------------------|--------------------------|--------------------------|
|  | 0.02 $\text{mL min}^{-1}$ | 0.2 $\text{mL min}^{-1}$ | 2.0 $\text{mL min}^{-1}$ |
| Motile (AW405)                         | $0.47 \pm 0.09$           | $0.70 \pm 0.08$          | $0.78 \pm 0.03$          |
| Nonmotile, paralyzed flagella (HCB136) | $0.76 \pm 0.07$           | $0.45 \pm 0.07$          | NR <sup>a</sup>          |
| Nonmotile, without flagella (HCB137)   | $0.80 \pm 0.06$           | $0.53 \pm 0.05$          | NR <sup>a</sup>          |

<sup>a</sup>Not reported. The number of bacteria that attached in these experiments was too small to determine an accurate  $F_R$ .



**Figure 3.** Normalized total bacterial concentration as a function of dimensionless time for AW405 (motile) (●), HCB136 (paralyzed) (■), and HCB137 (nonflagellate) (◆) for a flow rate of  $0.2 \text{ mL min}^{-1}$ . Each data point is an average of three experiments and the error is one standard deviation.

three bacterial strains ( $0.013 \pm 0.0007 \text{ cm h}^{-1}$ ,  $0.020 \pm 0.01 \text{ cm h}^{-1}$ , and  $0.016 \pm 0.004 \text{ cm h}^{-1}$  for motile, paralyzed, and nonflagellate bacterial strains, respectively; data not shown). The opposite trend was found for the  $F_R$  at this lower flow rate:  $0.47 \pm 0.09 \text{ cm h}^{-1}$ ,  $0.76 \pm 0.07 \text{ cm h}^{-1}$ , and  $0.80 \pm 0.06 \text{ cm h}^{-1}$  for motile, paralyzed, and nonflagellate bacterial strains, respectively (Table I).

Because both nonmotile species attached at a rate significantly higher than predicted by Eq. (4) (without kinetic limitation,  $J_{y,tot}/c_0$  for nonmotile bacteria would be  $0.0025 \text{ cm h}^{-1}$  and  $0.0053 \text{ cm h}^{-1}$  at  $0.02 \text{ mL min}^{-1}$  and  $0.2 \text{ mL min}^{-1}$ , respectively), this implies that attachment was not diffusion-limited and thus some other process was increasing the flux to the surface. We assumed the augmented attachment rate was the result of settling, because the theoretical and measured settling velocities were of the same order of magnitude as the total and net attachment rates. To test this, we measured the attachment rate of paralyzed bacteria to glass at a flow rate of  $0.2 \text{ mL min}^{-1}$  using buffer solutions of slightly higher densities. We chose glycerol concentrations that would increase the density of the bulk fluid to correspond to the range of densities reported for a single bacterium (Harvey, 1991). As the percentage of glycerol was increased, the density and viscosity of the fluid increased, which in turn decreased the settling velocity of nonmotile cells [Eq. (8)]. Thus, the total and net attachment rates decreased as the effect of settling was diminished (Fig. 4). In fact, using the cell density calculated from the measured settling velocity, we would predict attachment rates of  $0.014 \text{ cm h}^{-1}$  and  $0.006 \text{ cm h}^{-1}$  for the 10% and 20% glycerol solutions, respectively. Our experimental rates using the 10% and 20% glycerol solutions were  $0.012 \text{ cm h}^{-1}$  and  $0.0048 \text{ cm h}^{-1}$ , respectively. For motile cells, no significant difference was

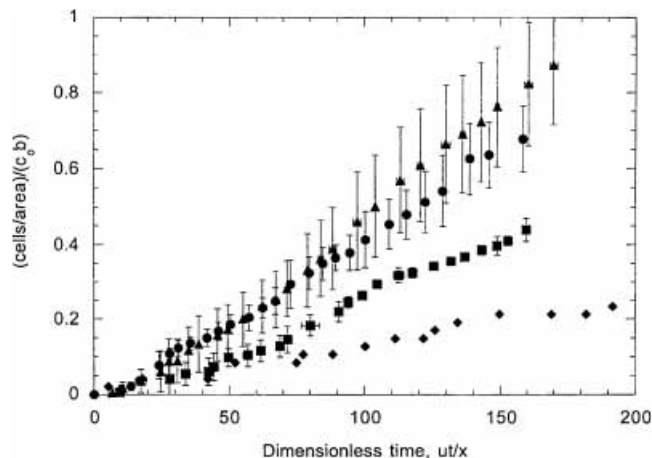


**Figure 4.** Normalized total bacterial concentration as a function of dimensionless time for HCB136 (paralyzed) at glycerol concentrations of 0% (v/v) (▲), 5% (v/v) (●), 10% (v/v) (■), and 20% (v/v) (◆). The densities and viscosities of the various solutions at  $20^\circ\text{C}$  are as follows: 0%,  $\rho_f = 0.998 \text{ g cm}^{-3}$ ;  $\mu = 0.00100 \text{ g cm}^{-1} \text{ s}^{-1}$ ; 5%,  $\rho_f = 1.010 \text{ g cm}^{-3}$ ,  $\mu = 0.00114 \text{ g cm}^{-1} \text{ s}^{-1}$ ; 10%,  $\rho_f = 1.022 \text{ g cm}^{-3}$ ,  $\mu = 0.00131 \text{ g cm}^{-1} \text{ s}^{-1}$ ; and 20%,  $\rho_f = 1.047 \text{ g cm}^{-3}$ ,  $\mu = 0.00177 \text{ g cm}^{-1} \text{ s}^{-1}$  (Perry and Green, 1984).

seen between 0%, 5%, and 10% glycerol solutions because attachment was dominated by diffusion to the surface (data not shown). Note that, at 20% glycerol, the motile cells stopped swimming.

We then tested the attachment of the three strains at a flow rate of  $2 \text{ mL min}^{-1}$  to minimize settling. At this velocity, the total and net attachment rates for motile cells was significantly higher than nonmotile cells (Fig. 5). For motile cells, we measured a  $J_{y,tot}/c_0$  of  $0.018 \pm 0.004 \text{ cm h}^{-1}$ , and for paralyzed and nonflagellate cells we measured attachment rates of  $0.0036 \pm 0.001 \text{ cm h}^{-1}$  and  $0.0037 \pm 0.002 \text{ cm h}^{-1}$ , respectively. Using Eq. (4), we then calculated the first-order adsorption rate con-

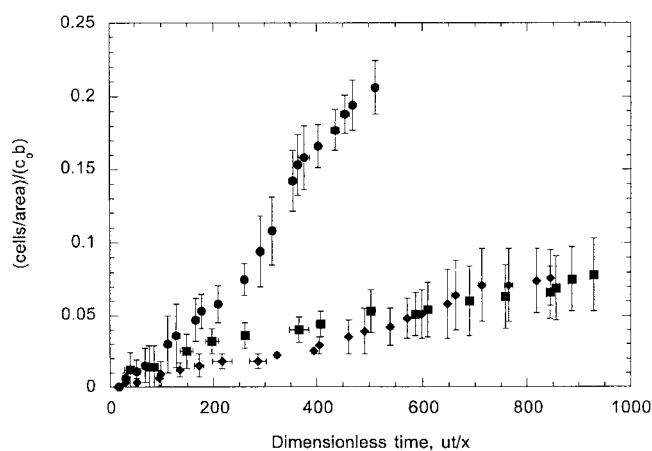


**Figure 5.** Normalized total bacterial concentration as a function of dimensionless time for AW405 (motile) (●), HCB136 (paralyzed) (■), and HCB137 (nonflagellate) (◆) for a flow rate of  $2.0 \text{ mL min}^{-1}$ . Each data point is an average of three experiments and the error is one standard deviation.

stants for each strain. For motile *E. coli*, the net and total adsorption rate constants were  $(3.3 \pm 0.49) \times 10^{-6} \text{ cm s}^{-1}$  and  $(4.1 \pm 0.38) \times 10^{-6} \text{ cm s}^{-1}$ , respectively, compared with  $(1.8 \pm 0.73) \times 10^{-6} \text{ cm s}^{-1}$  for paralyzed and  $(1.2 \pm 0.44) \times 10^{-6} \text{ cm s}^{-1}$  for nonflagellate bacteria (net and total were not distinguished because the number of bacteria that attached was not significant enough to determine an accurate  $F_R$ ). Because the adsorption rate constants for the three strains were of the same order of magnitude, this suggests that the difference in measured fluxes was diffusion-related. These values were similar to those reported by others (Camper et al., 1993; Mueller, 1996). Camper et al. measured attachment rate constants of  $6.5 \times 10^{-6} \text{ cm s}^{-1}$  and  $2.0 \times 10^{-6} \text{ cm s}^{-1}$  for motile and nonflagellate *P. fluorescens* to glass, respectively (Camper et al., 1993). Mueller et al. reported a value of  $5.1 \times 10^{-6} \text{ cm s}^{-1}$  for (motile) *P. aeruginosa* adhering to glass (Mueller, 1996).

Figure 6 shows the normalized total number of motile bacteria attached to glass as a function of dimensionless time for the three flow rates. As the flow rate was increased by an order of magnitude, the attachment rate decreased by roughly the same amount. The nondimensional total attachment rates,  $J_{y,\text{tot}}x/(ubc_o)$ , were  $(3.2 \pm 0.2) \times 10^{-2}$ ,  $(4.8 \pm 1) \times 10^{-3}$ , and  $(4.6 \pm 0.8) \times 10^{-4}$  for  $0.02 \text{ mL min}^{-1}$ ,  $0.2 \text{ mL min}^{-1}$ , and  $2 \text{ mL min}^{-1}$ , respectively.

## DISCUSSION

The attachment of bacteria to surfaces and subsequent formation of biofilms is important in many environmental, medical, and industrial processes. The present study has investigated the attachment of motile, paralyzed, and nonflagellate *E. coli* to glass surfaces under the influence of fluid flow to determine the specific role of flagella in dynamic adhesion. We were particularly

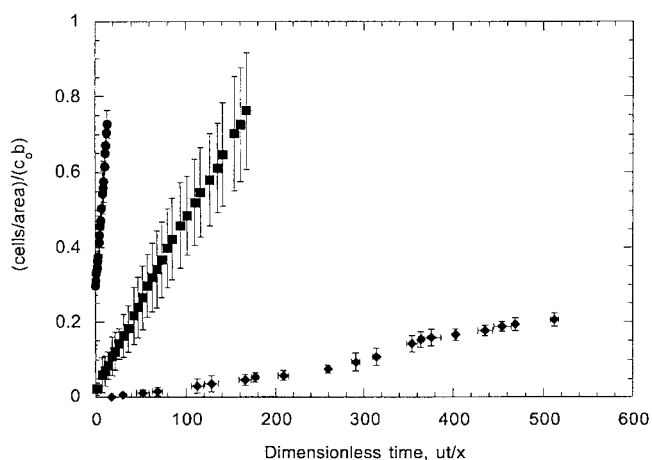


**Figure 6.** Normalized total bacterial concentration as a function of dimensionless time for AW405 (motile) at fluid velocities of  $0.02 \text{ mL min}^{-1}$  (●),  $0.2 \text{ mL min}^{-1}$  (■), and  $2 \text{ mL min}^{-1}$  (◆). Each data point is an average of three experiments and the error is one standard deviation.

interested in determining the range of fluid velocities in which motility became important in promoting non-specific attachment and detachment. We performed experiments with three *Escherichia coli* K12 strains: AW405 (motile, with flagella); HCB136 (nonmotile, with paralyzed flagella); and HCB137 (nonmotile, without flagella). Attachment and detachment rates were measured at flow rates of  $0.02 \text{ mL min}^{-1}$  ( $0.0044 \text{ cm s}^{-1}$ ),  $0.2 \text{ mL min}^{-1}$  ( $0.044 \text{ cm s}^{-1}$ ), and  $2 \text{ mL min}^{-1}$  ( $0.44 \text{ cm s}^{-1}$ ), which correspond to shear rates of  $0.34 \text{ s}^{-1}$ ,  $3.4 \text{ s}^{-1}$ , and  $34 \text{ s}^{-1}$ , respectively.

## Influence of Settling on Attachment Rate

The fluid velocities studied in this investigation are relevant to a variety of systems, including biomaterial environments (cardiovascular and urinary tract) and industrial applications. The lowest fluid velocity ( $0.0044 \text{ cm s}^{-1}$  or  $378 \text{ cm day}^{-1}$ ) is closest to typical interstitial groundwater velocities, which typically range between  $10 \text{ cm day}^{-1}$  and  $60 \text{ cm day}^{-1}$  for aquifers composed primarily of sand and gravel. Because this fluid velocity is on the order of typical cell swimming speeds, we expected the largest difference between total and net attachment rates of motile and nonmotile cells would be seen at this velocity. However, we discounted the importance of settling in transporting nonmotile cells to the surface at very low flow rates (Fig. 4). As can be seen in Figure 3, increasing the fluid velocity by an order of magnitude to  $0.2 \text{ mL min}^{-1}$  did not decrease the effect of settling, even though the average fluid velocity was several orders of magnitude greater than the settling velocity of a single bacterium. This emphasizes the importance of considering fluid streamlines close to the surface where velocities are approaching zero.

Figure 7 shows the trajectory of a single bacterium initially located at an arbitrary point ( $31 \mu\text{m}$ ) above the surface at the three fluid velocities, neglecting the effect of diffusion (according to Munn et al. [1994]). Figure 7 also shows the effect of settling decreases with increasing fluid velocity, but is still important at the two lowest fluid velocities used in this study. We would therefore also expect settling to be important at average velocities lower than experimental values (e.g., typical interstitial groundwater velocities). It should be noted that the presence of the solid surface will further reduce the axial velocity of the cells, but we did not include this in our illustration (Goldman et al., 1967).

## Diffusion and Settling Regimes

Adamczyk and van de Ven (1981) reported that sedimentation is important in particle deposition in flow chambers when the ratio of convective to diffusional transport is low. The relevant form of the Peclet number defined by Adamczyk and van de Ven (1981) is:

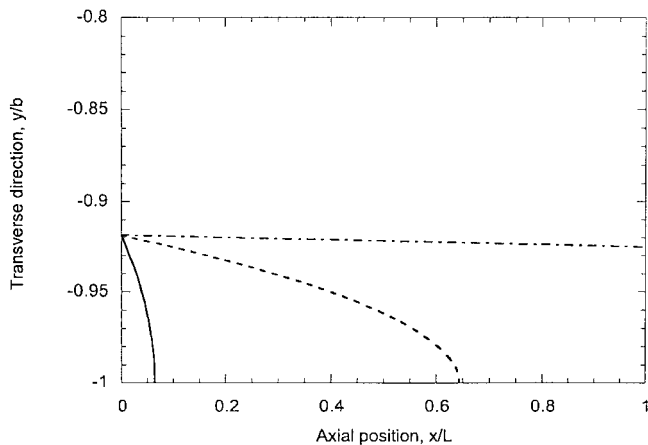


**Figure 7.** The trajectory of a bacterium initially located  $31\ \mu\text{m}$  above the glass surface ( $y/b = -0.92$ ) at the chamber inlet ( $x/L = 0$ ) for flow rates of  $0.02\ \text{mL min}^{-1}$  (—),  $0.2\ \text{mL min}^{-1}$  (---), and  $2\ \text{mL min}^{-1}$  (-·-). The effects of diffusion have been neglected for this illustration.

$$\text{Pe}_{av} = \frac{3ur_b^3}{2b^2D_b} \quad (9)$$

where for  $r_b$  is the radius of the bacterium.

Thus, for  $\text{Pe} \gg 1$ , the effects of sedimentation are small. Assuming a bacterial radius of about  $0.6\ \mu\text{m}$ , the Peclet numbers for our system are  $3.3 \times 10^{-4}$ ,  $3.3 \times 10^{-3}$ , and  $3.3 \times 10^{-2}$  for fluid velocities of  $0.0044\ \text{cm s}^{-1}$ ,  $0.044\ \text{cm s}^{-1}$ , and  $0.44\ \text{cm s}^{-1}$  (for nonmotile bacteria), and therefore, even at the highest fluid velocity, settling is still important (even though the attachment rate is significantly reduced for nonmotile bacteria). We apply this criterion to observations reported by several other investigators. Mueller et al. (1996) performed experiments in a chamber with a half-height of  $0.005\ \text{cm}$  and fluid velocity of  $2.75\ \text{cm s}^{-1}$ . Assuming their cells also had a radius of  $0.6\ \mu\text{m}$  and diffusion coefficient of  $3 \times 10^{-9}\ \text{cm}^2\ \text{s}^{-1}$ ,  $\text{Pe}_{av}$  is equal to 12 and we expect sedimentation to be unimportant. This is consistent with their results, in that they saw differences between the attachment rates of motile and nonmotile bacteria (Mueller, 1996). It therefore appears that for  $\text{Pe}_{av}$  approximately an order of magnitude higher than 1 (i.e., 10), sedimentation can be assumed negligible. Sjollem et al. (1988) reported a significant amount of sedimentation in experiments performed with various *Streptococci* strains. The conditions in their experiments were:  $b = 0.03\ \text{cm}$ ,  $u = 1.8\ \text{cm s}^{-1}$ ,  $D_b = 3$  to  $6 \times 10^{-9}\ \text{cm}^2\ \text{s}^{-1}$ , and  $a = 0.35$  to  $0.65\ \mu\text{m}$ . This corresponds to  $\text{Pe}_{av}$  ranging between 0.021 and 0.27.

Experiments performed by O'Toole and Kolter (1998a) measured the attachment of *Pseudomonas aeruginosa* to PVC in a stagnant system, thus  $\text{Pe}_{av} = 0$ . The dominant mechanism for transport to the surface should be settling for nonmotile strains and motility for the

motile strain (rates that were similar in magnitude in our experiments). However, they found that nonmotile strains (both with and without flagella) attached in much lower numbers to the PVC even after 8 h of incubation. Discrepancies between our experiments and those performed by O'Toole and Kolter could reflect differences in bacterial strains, surfaces tested, or experimental procedures. For example, if nonmotile cells did not attach as strongly as motile cells, then thorough and repeated rinsing of the surface (O'Toole and Kolter, 1998a) may have sheared off some of the nonmotile cells.

### Extension to Porous Material

We compared our results to colloid filtration theory, in which the attachment rate of colloidal particles to spherical collectors within a porous matrix is defined proportional to the collector efficiency (Rajagopalan and Tien, 1976; Yao et al., 1971). The collector efficiency is the ratio of the number of bacteria that strike a collector divided by the number of bacteria that flow toward the collector, and can be described by the following equation (Logan et al., 1995; Rajagopalan and Tien, 1976):

$$\eta = 4A_s^{1/3} \left( \frac{u^* d_c}{D_b} \right)^{-2/3} + A_s N_{Lo}^{1/8} N_R^{15/8} + 0.00338 A_s \left( \frac{v_s}{u^*} \right)^{1.2} N_R^{-0.4} \quad (10)$$

where  $A_s$  is the Happel correction factor that accounts for the proximity of the collectors,  $u^*$  is the superficial fluid velocity,  $d_c$  is the diameter of the collector,  $N_{Lo}$  is a dimensionless number that represents the contribution of London-van der Waals attractive forces, and  $N_R$  is the interception number,  $d_b/d_c$ , where  $d_b$  is the diameter of a bacterium.

The terms on the right-hand side of Eq. (10) represent the effects of diffusion, interception plus London-van der Waals forces, and settling plus interception, respectively. If we assume a collector diameter equal to the chamber height ( $0.0762\ \text{cm}$ ), a Happel correction factor of 75 (assumes a porosity  $[\theta]$  of 0.3; see Logan et al. [1995] for definition of  $A_s$ ), and a bacterium diameter of  $1\ \mu\text{m}$ , we can compare the relative importance of the first and third terms in this equation for the conditions of our experiments as they might apply to porous media. For motile bacteria over the range of fluid velocities tested in this study, the first term is always dominant, which means bacteria primarily transport to the surface by diffusion (this is true even if we assume a settling velocity equal to that of nonmotile cells). For nonmotile bacteria, the first and third terms are of the same order of magnitude for  $0.0044\ \text{cm s}^{-1}$  (0.007 and 0.002, respectively), indicating that settling and diffusion are

equally important. For  $0.044 \text{ cm s}^{-1}$ , the diffusional term (0.0016) is one order of magnitude higher than the settling term (0.00012), and at  $0.44 \text{ cm s}^{-1}$ , the terms differ by two orders of magnitude ( $3.4 \times 10^{-4}$  and  $7.9 \times 10^{-6}$ ). Thus, settling is much more important at the two lowest fluid velocities tested in this study. Assuming a Hamaker constant of  $10^{-20} \text{ J}$  (Logan et al., 1995), we estimate the collector efficiencies for nonmotile bacteria at 0.0044, 0.044, and  $0.44 \text{ cm s}^{-1}$  to be  $9.4 \times 10^{-3}$ ,  $1.8 \times 10^{-3}$ , and  $4.5 \times 10^{-4}$ , respectively. For motile bacteria, collector efficiencies were calculated as 0.71, 0.15, and 0.033 at 0.0044, 0.044, and  $0.44 \text{ cm s}^{-1}$ , respectively.

Therefore, according to colloid filtration theory, settling and diffusion are of approximately equal importance in attachment at the two lower fluid velocities for nonmotile cells in porous media. In our experimental system, settling must have been more dominant than diffusion at the low fluid velocities because we observed that transport to the surface was approximately the same for both motile and nonmotile species. At the highest flow rate, the importance of settling was considerably less (Fig. 5). The total attachment rate of motile bacteria was approximately five times higher than that of both nonmotile strains at  $2.0 \text{ mL min}^{-1}$ . Differences in dominant transport mechanisms between our data and colloid filtration theory reflect the different experimental geometries. Furthermore, because the gravitational number is defined as the ratio of the settling velocity to the fluid velocity, the importance of settling may be masked by the much larger value of the fluid velocity.

### Comparison of Fractions Retained

The fraction of motile and nonmotile bacteria retained on the glass surfaces was significantly different for flow rates of  $0.02 \text{ mL min}^{-1}$  and  $0.2 \text{ mL min}^{-1}$ . For motile bacteria, the fraction of bacteria retained on the surface increased with fluid velocity (Table I). This effect was most significant in comparing data at the two lower flow rates. For the two nonmotile strains, the fractions retained decreased with increasing flow rate. A similar effect was found by Camesano and Logan measuring the fraction of motile and nonmotile (with flagella) *Pseudomonas fluorescens* P17 retained in soil columns at pore velocities ranging between  $0.00065$  and  $0.14 \text{ cm s}^{-1}$  (Camesano and Logan, 1998). The fraction of motile cells retained on the soil particles increased significantly between  $6.5 \times 10^{-4}$  and  $0.0625 \text{ cm s}^{-1}$ , and became relatively constant above  $0.0625 \text{ cm s}^{-1}$ . The fraction of nonmotile cells retained in the column decreased with velocity under identical conditions, as predicted by colloid filtration theory (Yao et al., 1971). It should be noted that Camesano and Logan (1998) defined their fraction retained as the amount of cells that remain at-

tached to the soil particles at the end of an experiment (attached cells/total injected cells):

$$F_{R,cf} = \left(1 - \frac{c}{c_0}\right) = 1 - \exp\left[-\frac{3(1-\theta)}{2} \frac{\eta\alpha L}{d_c}\right] \quad (11)$$

where  $\alpha$  is the collision (or sticking) efficiency, defined as the rate at which cells attach to a collector divided by rate at which cells strike a collector, and  $L$  is the column length.

This is slightly different from our definition (we divided the net attached cells by the total cells that have attached rather than by  $c_0$ ). Both definitions would give the same trends, but results are attributed to different physical mechanisms. Specifically, measurement of  $F_{R,cf}$  in soil columns does not differentiate between transport and adsorption effects ( $\eta$  vs.  $\alpha$ ); however, a sticking efficiency can be determined from experimental data using Eq. (10) to calculate  $\eta$  and knowing all other parameters. Furthermore it is assumed that cell detachment is relatively small and is not included. Our definition of the fraction retained also contains transport and adsorption, as well as cell detachment.

We suggest the mechanism for detachment is responsible for the differences in fractions retained between the motile and nonmotile bacteria. Specifically, nonmotile cells primarily detached as the result of shear, so that increasing the flow rate increased the amount of cells that detached. For motile cells, we believe the movement of the flagella may enable bacteria to detach from the surface (at low flow rates) or have the reverse effect and strengthen the attachment by more flagellar interaction (at high flow rates). In experiments, motile (and nonmotile) bacteria typically attached to the glass at some point on the cell body (i.e., very few cells tethered by flagella were seen). At the two higher flow rates, we saw many cases where attached nonmotile cells (both paralyzed and nonflagellate) moved about  $15 \mu\text{m}$  in the direction of flow during the course of the experiment ( $\sim 1.5 \text{ h}$ ). This did not happen at all for the motile cells, which suggests that both nonmotile species were not held to the surface as strongly as the motile bacteria. Thus, we assume the movement of the flagella facilitated additional attachments to anchor the cell to the surface.

We did not observe any difference in the fractions of paralyzed and nonflagellated cells retained on the glass surfaces for the range of fluid velocities studied. This suggests that the presence of flagella alone does not influence initial attachment events, although they may be important in later stages of biofilm formation. This is similar to results reported by others (Korber et al., 1994; Watnick and Kolter, 1999). The initial attachment rate of nonmotile *P. fluorescens* to glass surfaces was the same for both heat-treated (motile cells rendered nonmotile) and nonflagellated bacteria at a fluid velocity of  $0.37 \text{ cm s}^{-1}$  (Korber et al., 1994). Watnick and Kolter reported no difference in the rate of biofilm formation

between *V. cholerae* El Tor mutants with a paralyzed flagellum and mutants without a flagellum at all (Watnick and Kolter, 1999).

## CONCLUSIONS

A technique was developed to measure the initial attachment and detachment of bacteria to glass surfaces for various fluid velocities. We performed experiments with *E. coli* AW405 (motile), *E. coli* HCB136 (nonmotile mutant with flagella), and *E. coli* HCB137 (nonmotile mutant without flagella) to better characterize the role of flagella in bacterial adhesion in dynamic systems. We report the following conclusions from this research.

The transport of motile bacteria to surfaces is dominated by diffusion, whereas nonmotile bacterial transport is dominated by settling at low fluid velocities, and by Brownian diffusion at high velocities. Furthermore, the transport of motile bacteria to surfaces by diffusion is of the same order of magnitude as the settling of nonmotile bacteria. Motility was therefore advantageous to bacterial adhesion only at higher fluid velocities for the conditions of these experiments. Thus, in interpreting experimental data it is important to discern whether settling is a factor for the given experimental conditions.

The presence of flagella did not appear to have an effect on the initial attachment rate of nonmotile bacteria. However, the movement of the flagella enabled attached (motile) bacteria to detach at low flow rates, and appeared to strengthen adhesion at high flow rates.

The adhesion of bacteria to surfaces is the first stage in biofilm formation. It is therefore necessary to understand this process to be better able to promote or impede biofilm development in various systems. Although we have emphasized the application of this work to bioremediation, results from this research can be applied to many fields and will enhance our understanding of bacterial attachment to surfaces.

The authors thank Howard Berg for the *E. coli* strains. We are grateful to Jeff DiVietro and Michael Lawrence, Department of Biomedical Engineering, University of Virginia, for their design of the parallel-plate flow chamber.

## NOMENCLATURE

|       |                              |                           |
|-------|------------------------------|---------------------------|
| $a_b$ | bacteria half-height         | (cm)                      |
| $A_s$ | Happel correction factor     |                           |
| $A_v$ | viewing area                 | (cm <sup>2</sup> )        |
| $b$   | chamber half-height          | (cm)                      |
| $b_b$ | bacteria half-width          | (cm)                      |
| $c$   | bacterial concentration      | (cells cm <sup>-3</sup> ) |
| $c_o$ | bulk bacterial concentration | (cells cm <sup>-3</sup> ) |
| $d_b$ | diameter of a bacterium      | (cm)                      |
| $d_c$ | diameter of a collector      | (cm)                      |

|                  |  |   |
|------------------|--|---|
| $D_b$            | diffusion or random motility coefficient   | (cm <sup>2</sup> s <sup>-1</sup> )        |
| $f$              | friction factor  |   |
| $F_R$            | fraction retained, equal to $J_{y,net}/J_{y,total}$  |   |
| $F_{R,cf}$       | fraction retained as defined by colloid filtration theory                                    |   |
| $g$              | gravitational constant, 981 cm s <sup>-2</sup>   |   |
| $J_y$            | bacterial flux to surface  | (cells cm <sup>-2</sup> s <sup>-1</sup> ) |
| $J_{y,net}$      | net bacterial flux to surface  | (cells cm <sup>-2</sup> s <sup>-1</sup> ) |
| $J_{y,tot}$      | total bacterial flux to surface  | (cells cm <sup>-2</sup> s <sup>-1</sup> ) |
| $J_{y,tot}/c_o$  | total attachment rate  | (cm s <sup>-1</sup> )                     |
| $k$              | Boltzmann constant, $1.38 \times 10^{-16}$ g cm <sup>2</sup> s <sup>-2</sup> K <sup>-1</sup> |   |
| $k_a$            | first-order adsorption rate constant   | (cm s <sup>-1</sup> )                     |
| $L$              | column length  | (cm)                                      |
| $N_b$            | number of bacteria   | (cells)                                   |
| Pe               | Peclet number  |   |
| Pe <sub>av</sub> | Peclet number according to Adamczyk and van de Ven (1981)                                    |   |
| $r_b$            | radius of a spherically shaped bacterium   | (cm)                                      |
| $t$              | time   | (s)                                       |
| $T$              | absolute temperature   | (K)                                       |
| $u$              | average fluid velocity   | (cm s <sup>-1</sup> )                     |
| $u^*$            | superficial velocity (porous media)  | (cm s <sup>-1</sup> )                     |
| $v$              | fluid velocity (parabolic profile)   | (cm s <sup>-1</sup> )                     |
| $V$              | volume of a bacterium  | (cm <sup>3</sup> )                        |
| $v_s$            | settling velocity  | (cm s <sup>-1</sup> )                     |
| $x, y$           | axial and transverse directions, respectively  | (cm)                                      |
| $\alpha$         | collision (or sticking) efficiency   |   |
| $\gamma$         | nondimensional term, equal to $(l/Pe)$ ( $8x/3b$ )   |   |
| $\Gamma$         | the gamma function, $\Gamma(4/3) = 0.89338$  |   |
| $\eta$           | collector efficiency   |   |
| $\lambda$        | settling correction factor   |   |
| $\rho_s$         | density of a bacterium   | (g cm <sup>-3</sup> )                     |
| $\rho_f$         | density of the fluid   | (g cm <sup>-3</sup> )                     |
| $\mu$            | fluid viscosity  | (g cm <sup>-1</sup> s <sup>-1</sup> )     |
| $\theta$         | porosity   |   |

## References

- Adamczyk Z, van de Ven TGM. 1981. Deposition of particles under external forces in laminar flow through parallel-plate and cylindrical channels. *J Coll Inter Sci* 80:340–356.
- Aizawa S-I. 1996. Flagellar assembly in *Salmonella typhimurium*. *Mol Microbiol* 19:1–5.
- Berg HC. 1993. *Random walks in biology*. Princeton, NJ: Princeton University Press.
- Bird RB, Stewart WE, Lightfoot EN. 1960. *Transport phenomena*. New York: John Wiley & Sons.
- Bowen BD, Levine S, Epstein N. 1976. Fine particle deposition in laminar flow through parallel-plate and cylindrical channels. *J Coll Inter Sci* 54:375–390.
- Brenner H. 1961. The slow motion of a sphere through a viscous fluid towards a plane surface. *Chem Eng Sci* 16:242–251.
- Camesano TA, Logan BE. 1998. Influence of fluid velocity and cell concentration on the transport of motile and non-motile bacteria in porous media. *Environ Sci Technol* 32:1699–1708.
- Camper AK, Hayes JT, Sturman PJ, Jones WL, Cunningham AB. 1993. Effects of motility and adsorption rate coefficient on transport of bacteria through saturated porous media. *Appl Environ Microbiol* 59:3455–3462.
- Characklis WG, Marshall KC. 1990. Modeling the initial events in biofilm accumulation. In: Characklis WG, Marshall KC, editors. *Biofilms*. New York: John Wiley & Sons. p 3–15.
- Costerton JW, Cheng K-J, Geesey GG, Ladd TI, Nickel JC, Dasgupta M, Marrie TJ. 1987. Bacterial biofilms in nature and disease. *Ann Rev Microbiol* 41:435–464.

- Dickinson RB, Cooper SL. 1995. Analysis of shear-dependent bacterial adhesion kinetics to biomaterial surfaces. *AIChE J* 41:2160–2174.
- Feldman M, Bryan R, Rajan S, Scheffler L, Brunnert S, Tang H, Prince A. 1998. Role of flagella in pathogenesis of *Pseudomonas aeruginosa* pulmonary infection. *Infect Immun* 66:43–51.
- Gannon JT, Manilal VB, Alexander M. 1991. Relationship between cell surface properties and transport of bacteria through soil. *Appl Environ Microbiol* 57:190–193.
- Goldman AJ, Cox RG, Brenner H. 1967. Slow viscous motion of a sphere parallel to a plane wall—II. Couette flow. *Chem Eng Sci* 22:653–660.
- Gristina AG. 1987. Biomaterial-centered infection: Microbial adhesion versus tissue integration. *Science* 237:1588–1595.
- Gross MJ, Logan BE. 1995. Influence of different chemical treatments on transport of *Alcaligenes paradoxus* in porous media. *Appl Environ Microbiol* 61:1750–1756.
- Harvey RW. 1991. Parameters involved in modeling movement of bacteria in groundwater. In: Hurst CJ, editor. *Modeling the environmental fate of microorganisms*. Washington, DC: American Society for Microbiology p 89–114.
- Hobbie JE, Daley RJ, Jasper S. 1977. Use of nucleopore filters for counting bacteria by fluorescence microscopy. *Appl Environ Microbiol* 33:1225–1228.
- Korber DR, Lawrence JR, Caldwell DE. 1994. Effect of motility on surface colonization and reproductive success of *Pseudomonas fluorescens* in dual-dilution continuous culture and batch culture systems. *Appl Environ Microbiol* 60:1421–1429.
- Lawrence JR, Delaquis PJ, Korber DR, Caldwell DE. 1987. Behavior of *Pseudomonas fluorescens* within the hydrodynamic boundary layers of surface microenvironments. *Microb Ecol* 14:1–14.
- Lewus P, Ford RM. 2001. Quantification of random motility and chemotaxis bacterial-transport coefficients using individual-cell and population-scale assays. *Biotechnol Bioeng* 75:292–304.
- Logan BE, Jewett DG, Arnold RG, Bouwer EJ, O'Melia CR. 1995. Clarification of clean-bed filtration models. *J Environ Eng* 121:869–873.
- Macnab RM. 1996. Flagella and motility. In: Neidhardt FC, editor. *Escherichia coli and Salmonella cellular and molecular biology*. Washington, DC: ASM Press. p 123–145.
- McMurtry DC, Elton RO. 1985. New approach to *in-situ* treatment of contaminated groundwaters. *Environ Prog* 4:168–170.
- Meinders JM, Noordmans J, Busscher HJ. 1992. Simultaneous monitoring of the adsorption and desorption of colloidal particles in a parallel plate flow chamber. *J Coll Inter Sci* 152:265–280.
- Meinders JM, van der Mei HC, Busscher HJ. 1994. Physicochemical aspects of deposition of *Streptococcus thermophilus* B to hydrophobic and hydrophilic substrata in a parallel plate flow chamber. *J Coll Interf Sci* 164:355–363.
- Mohamed N, Rainier TR, Ross JM. 2000. Novel experimental study of receptor-mediated bacterial adhesion under the influence of fluid shear. *Biotechnol Bioeng* 68:628–636.
- Mohamed N, Teeters MA, Patti JM, Höök M, Ross JM. 1999. Inhibition of *Staphylococcus aureus* adherence to collagen under dynamic conditions. *Infect Immun* 67:589–594.
- Mueller RF. 1996. Bacterial transport and colonization in low nutrient environments. *Water Res* 30:2681–2690.
- Munn LL, Melder RJ, Jain R. 1994. Analysis of cell flux in the parallel plate flow chamber: implications for cell capture. *Biophys J* 67:889–895.
- O'Toole GA, Kolter R. 1998a. Flagellar and twitching motility are necessary for *Pseudomonas aeruginosa* biofilm development. *Mol Microbiol* 30:295–304.
- O'Toole GA, Kolter R. 1998b. Initiation of biofilm formation in *Pseudomonas fluorescens* WCS365 proceeds via multiple, convergent signalling pathways: A genetic analysis. *Mol Microbiol* 28:449–461.
- Perry RH, Green DW, editors. 1984. *Perry's chemical engineers' handbook*. New York: McGraw-Hill.
- Pratt LA, Kolter R. 1998. Genetic analysis of *Escherichia coli* biofilm formation: Roles of flagella, motility, chemotaxis, and type I pili. *Mol Microbiol* 30:285–293.
- Rajagopalan R, Tien C. 1976. Trajectory analysis of deep-bed filtration with the sphere-in-cell porous media model. *AIChE J* 22: 523–533.
- Sjollem J, Busscher HJ, Weerkamp AH. 1988. Deposition of oral streptococci and polystyrene latices onto glass in a parallel plate flow chamber. *Biofouling* 1:101–112.
- Starr RC, Cherry JA. 1994. In situ remediation of contaminated groundwater: The funnel-and-gate system. *Groundwater* 32:465–476.
- Vatanyoopaisarn S, Nazli A, Dodd CER, Rees CED, Waites WM. 2000. Effect of flagella on initial attachment of *Listeria monocytogenes* to stainless steel. *Appl Environ Microbiol* 66:860–863.
- Watnick PI, Kolter R. 1999. Steps in the development of *Vibrio cholerae* El Tor biofilm. *Mol Microbiol* 34:586–595.
- Witt ME, Dybas MJ, Worden RM, Criddle CS. 1999. Motility-enhanced bioremediation of carbon tetrachloride-contaminated aquifer sediments. *Environ Sci Technol* 33:2958–2964.
- Wollum AG, Cassel DK. 1978. Transport of microorganisms in sand columns. *Soil Sci Soc Am J* 42:72–76.
- Yao KM, Habibian MT, O'Melia CR. 1971. Water and waste water filtration: Concepts and applications. *Environ Sci Technol* 11:1105–1112.